Bulletin de la Société Royale des Sciences de Liège, Vol. 86, *special issue,* 2017, *p.* 139 - 156

CO_2/CH_4 Sorption Behavior of Glassy Polymeric Membranes Based on Dual Mode Sorption Model

Mohammad ASKARI[1,*]

[1] Research Institute of Petroleum Industry (RIPI), West Blvd. Azadi Sport Complex, Tehran, Iran, 1485733111
[*]Corresponding Author's Email: askarim@ripi.ir

Abstract

Among the various transport models for gas separation via membrane, the best description is done by solution-diffusion model. The main parameters of this model are the sorption and diffusion of the penetrant through the membrane. Studies conducted by various researchers in the field of gas separation indicate that the thermodynamic interaction (sorption effects) in glassy polymers has the major role in the diffusivity, permeability, and selectivity of the membrane, especially in the multi-component gas mixture. In glassy polymers, dual-mode sorption model is frequently used to describe the equilibrium sorption behavior of a polymer-gas system and, based on this sorption model; the permeation behavior is described by the partial immobilization model. In this study, the difference between the sorption mechanism of CO_2 and CH_4 in glassy polymeric membranes was analyzed by separating the sorption mode and introducing $P_{50/50}$ parameter (the pressure at which the contribution of both Henry and Langmuir sorption is equal), which was done using the available experimental data in the scientific references for the sorption values of CO_2 and CH_4. The contribution of the sorbed molecules in Henry and Langmuir sites was investigated and its changes with pressure were evaluated for CO_2 and CH_4 permeation. This study was also attempted to provide a correct definition of F factor, used in references, in the form of the multiplication of mobile concentration ratios ($C_{Hmobile}/C_H$) by the diffusivity coefficients in two modes (D_H/D_D).

Keywords: Glassy polymer, Permeability coefficient, Dual-mode sorption model, Partial immobilization model

1. Introduction

The usage of natural gas as a clean and efficient fuel is constantly growing around the world. In addition, methane as the main component of natural gas is considered a principal feedstock for petrochemical and chemical industries. At present, natural gas purification is one of the most important industrial gas separation processes. In this process, acid gas (CO_2, H_2S, and mercaptans), mainly CO_2, is removed from natural gas [1-5].

Pressure swing adsorption (PSA), the absorption of acid gases in solvents (such as dimethylamine or diethylamine solutions), and the membrane process are some examples of natural gas purification technologies [4-6].

Recently, membrane separation has received great attention due to its high-energy efficiency, ease of scale-up, and being environmentally friendly. A variety of polymers has been synthesized as membranes and investigated for gas separation applications. Among these materials, glassy polymers (such as polyimides, polysulfone, and polycarbonate) are among the most attractive and favorable materials as a result of some admirable properties such as high thermal stability, mechanical strength, chemical resistance, and spinnability [1, 4-12].

Gas transport across a polymeric membrane mainly follows the solution-diffusion mechanism, in which permeability is affected by solubility and diffusivity coefficients [13-17]. In this mechanism, a gas molecule is sorbed onto the membrane surface, then diffuses across the polymer medium, and subsequently is desorbed from the other face of the membrane. Therefore, both kinetic factors, like segment mobility and free volume, which are mostly dependent on the penetrant size, and thermodynamic factors, like condensability of the gas and its interaction with polymer segments, can affect the permeation process [17].

The effects of pressure and concentration of penetrant molecules are crucial in gas transport modeling. As can be seen in Figure 1 and Figure 2, the effect of pressure on permeability and solubility can be divided into four conditions. The first one shown in Figure 1.a and Figure 2.a regards sorption and diffusion as independent from the gas pressure, which is proper for ideal conditions. This case is applied for the sorption and permeation of supercritical gases in amorphous polymers and can be defined by Henry's law. The second case shown in Figure 1.b and Figure 2.b is useful for the sorption and permeation of organic compounds in elastic polymers. In this case, due to the fineness and flexibility of these kinds of polymers, sorption and permeation are enhanced by increasing the pressure. The third case shown in Figure 1.c and Figure 2.c is applied for the sorption and permeation of gases with high solubility in glassy polymers without the plasticization behavior. In this case, sorption obeys the dual-mode sorption model. The last case shown in Figure 1.d and Figure 2.d is relevant for the sorption and permeation of highly condensable gases in glassy polymers with the plasticization effect.

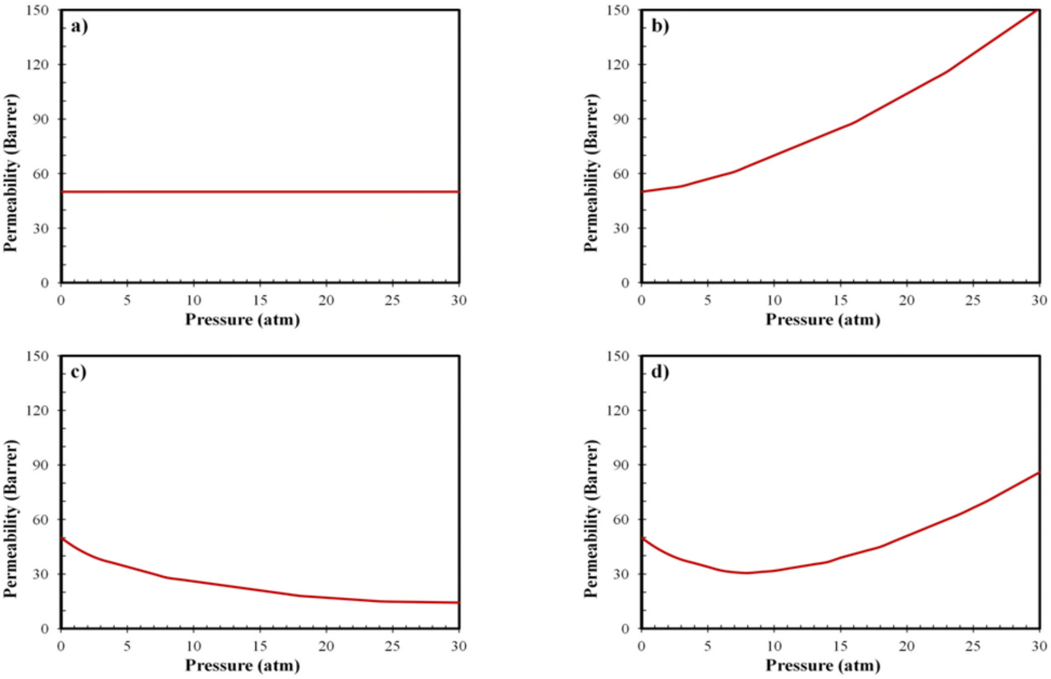

Fig.1: Effect of pressure on permeability in four conditions a) Ideal b) organic compound in elastic polymers c) High solubility gases in glassy polymers without plasticization behavior d) Highly condensable gases in glassy polymers with plasticization effect

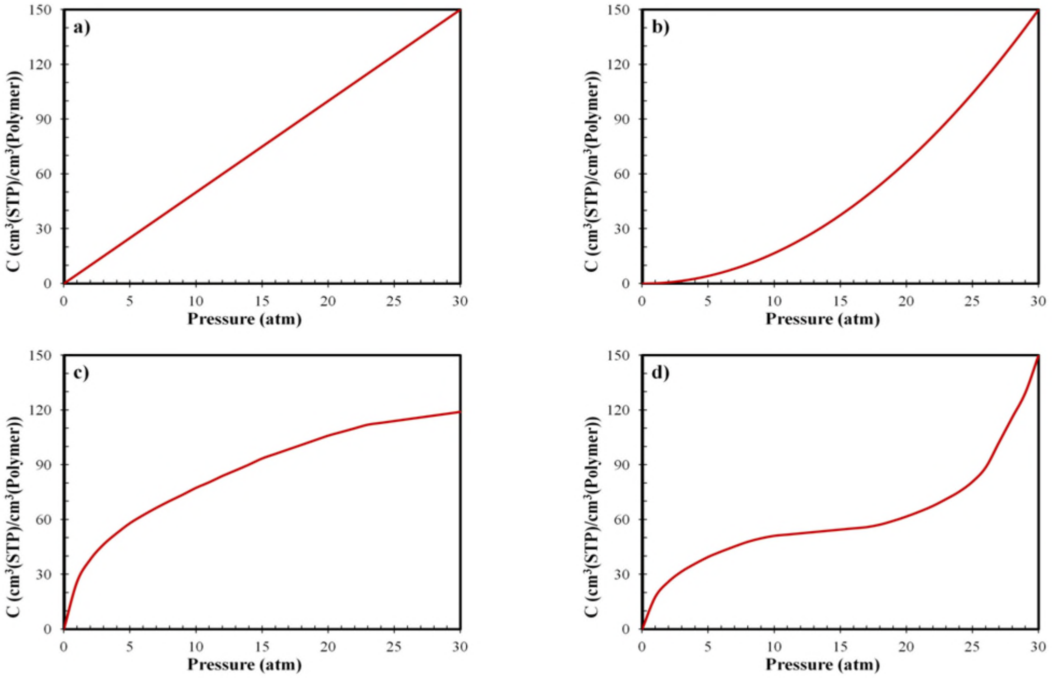

Fig.2: Effect of pressure on solubility in four conditions a)Ideal b) organic compound in elastic polymers c) High solubility gases in glassy polymers without plasticization behavior d) Highly condensable gases in glassy polymers with plasticization effect

Researchers have found that the effect of the thermodynamic factor (sorption) is more crucial than that of the kinetic factor (diffusion) in gas permeability and selectivity. Then, the sorption behavior of gases in glassy polymers can be a key factor to select the polymer for the mixed gas separation [5, 16-28]. In this study, we summarized the sorption behavior of CO_2 and CH_4 in a variety of glassy polymers, as listed in Table 1, and explained the difference between the sorption behaviors of these polymers. For this propose, we defined a pressure that has the same sorption in Henry and Langmuir sites as $P_{50/50}$ and also calculated the gas sorption in Henry and Langmuir site for each polymer.

Table 1: List of selected glassy polymers

Polymer	Condition	Designation	T (°C)	Press. (atm)	Ref.
6FDA-DAM/DABA (3/2)	Treat @ 180 °C, 18 h	CPI1-180	35	7	[1]
	Treat @ 230 °C, 18 h	CPI1-230	35	7	[1]
6FDA-bisAPAF	Treat @ 300 °C, 1 h	6F-bisAPAF-300	35	1	[5]
	Treat @ 350 °C, 1 h	6F-bisAPAF-350	35	1	[5]
	Treat @ 400 °C, 1 h	6F-bisAPAF-400	35	1	[5]
	Treat @ 450 °C, 1 h	6F-bisAPAF-450	35	1	[5]
PIM-1	Casting In Chloroform	PIM-1	25	1	[16]
Polyphenylene Oxide (PPO)	Original	PPO	35	10	[18]
	Carboxylated PPO	CPPO	35	10	[18]
	Methyl esterified CPPO	MeCPPO	35	10	[18]
	Brominated PPO	BPPO	35	10	[18]
Polystyrene		PS	35	10	[19,20]
6FDA-Durene/DABA (9/1)	Treat @ 200 °C, 2 h	CPI2-200	35	1	[21]
	Treat @ 425 °C, 2 h	CPI2-425	35	1	[21]
	Grafted γ-CD & Treat @ 200 °C, 2 h	CPI2-g-γ-CD-200	35	1	[21]

	Grafted γ-CD & Treat @ 425 °C, 2 h	CPI2-g-γ-CD-425	35	1	[21]
6FDA-6FpDA		6F-6FpDA	35	10	[22]
6FDA-1,5-NDA		6F-1,5-NDA	35	10	[23]
Polysulfone (PSF)	Original	PSF	30	10	[24]
	Dimethyl Polysulfone	DMPSF	30	10	[24]
	Brominated Polysulfone	BPSF	30	10	[25]
	Trimethylsilylated Polysulfone	TMSPSF	30	10	[25]
Polycarbonate		PC	35	10	[26]
Polyhydroxyether		PH	35	10	[27]
Polyetherimide		PEI	35	10	[27]
Polyarylate		PA	35	10	[27]
Polycarbonate		PC	35	10	[27]
6FDA-TADPO polypyrrolone		6F-TADPO	35	10	[40]
Bromo Trimethylsilylated polysulfone		BTMSPSF	30	10	[41]
6FDA-HAB		6F-HAB	35	10	[42,43]
	TR 350 °C, 1 h	6F-HAB-TR-350	35	10	[42,43]
	TR 400 °C, 1 h	6F-HAB-TR-400	35	10	[42,43]
	TR 450 °C, 0.5 h	6F-HAB-TR-450	35	10	[42,43]
Ultem®1000		Ultem	35	3.5	[44,45]
Matrimid®5218		Matrimid	35	3.5	[44,45]
Poly (1-trimethylsilyl-1-propyne)	Casting in THF	PTMSP	35	1	[46,47]

2. Theory and background

2.1 Dual-Mode Sorption Model

Gas transport through glassy polymeric membranes is frequently described by the dual-mode sorption model. The Henry sorption is the main mechanism of transporting sorption to the matrix component and is defined by C_D, while the Langmuir sorption governs the sorption into the micro-void region and is defined by C_H. Therefore, total sorption (C) is written as:

$$C = C_D + C_H = k_D p + \frac{C'_H bp}{1+bp} \tag{1}$$

where C is the concentration of the gas sorbed in the polymer with a unit of gas volume (cm^3) per polymer volume (cm^3), p (atm) is the pressure of the feed gas in contact with the polymer, k_D is the Henry's law constant indicating gas dissolution into the equilibrium-defined polymer matrix, C'_H is the Langmuir capacity of the glassy polymer that is related to the un-relaxed volume, which is a measure of the departure from equilibrium in the glassy state, and b is the Langmuir affinity parameter describing the affinity of the gas to a Langmuir site. The Langmuir capacity can be viewed as a measurement of the excess free volume of a polymer [16-18, 29-31]. Solubility coefficient (S) of a gas in a glassy polymeric membrane is described as the ratio of the equilibrium gas concentration to the applied gas pressure, as written in Eq. (2).

$$S = \frac{C}{p} = k_D + \frac{C'_H b}{1+bp} \tag{2}$$

Gas sorption may display an unusual isotherm if a gas is polar in nature and highly condensable. Since gas sorption isotherm can be experimentally performed, the three dual-mode sorption parameters (k_D, C'_H, and b) can be obtained by the curve fitting using a nonlinear least squares method [32-38].

2.2 Partial Immobilization Model

In the dual-mode sorption theory, the Langmuir mode species is originally considered not to be mobile at all [31]. In contrast, the partial immobilization model is based on the independent dual diffusion of the Henry and Langmuir modes, but assumes that the species in the Langmuir mode can relatively mobilize in glassy polymeric membranes. Since the concentration C of the gas sorption is assumed to obey the dual-mode sorption model as written by Eq. (1), permeation flux (permeation amount per unit time) J and permeability coefficient P through the glassy polymeric membrane can be written by Eq. (3) and Eq. (4), respectively [21, 31-32].

$$J = -D(C)\frac{\partial C}{\partial y} = -D_D\frac{\partial C_D}{\partial y} - D_H\frac{\partial C_H}{\partial y} = -D_D\left(1+\frac{FK}{(1+bp)^2}\right)\frac{\partial C_D}{\partial y} = -D_D\left(\frac{1+\frac{FK}{(1+bp)^2}}{1+\frac{K}{(1+bp)^2}}\right)\frac{\partial C}{\partial y} \tag{3}$$

$$P = S\times D = \frac{C}{p}\times D = k_D\left(1+\frac{K}{1+bp}\right)\times D = k_D D_D + \frac{C'_H b D_H}{1+bp} = k_D D_D\left(1+\frac{FK}{1+bp}\right) \tag{4}$$

where C is the concentration of the penetrant, y is the membrane thickness, $D(C)$ is the concentration-dependent diffusion coefficient, D_D is the diffusion coefficient under the Henry mode, D_H is the diffusion coefficient under the Langmuir mode, F is the ratio of the two diffusion coefficients (D_H/D_D), K is equal to bC'_H/k_D, D is the average diffusion coefficient, and P is the average permeability coefficient. The permeability coefficient, P, decreases slowly with an increase in the system pressure and, then, reaches $k_D D_D$, irrespective of the F value because of the saturation of Langmuir sites. For the binary gas mixture, dual-mode sorption model can be developed. For this purpose, Henry constant for each gas can be assumed independent and uninfluenced by other gases and the pressure of the permeate side for both gases is zero. For the binary gas mixture, total sorption of gasses in polymer and permeability of gas A can be written by Eq. (5) and Eq. (6), respectively [1, 24-25, 33].

$$C = k_{D_A} p_A + k_{D_B} p_B + \frac{C'_{H_A} b_A p_A + C'_{H_B} b_B p_B}{1+b_A p_A + 1+b_B p_B} \tag{5}$$

$$P_A = k_{D_A} D_{D_A}\left(1+\frac{F_A K_A}{1+b_A p_A + b_B p_B}\right) \tag{6}$$

where p_A and p_B are partial pressures of gases A and B in the polymer, respectively.

3. Results and discussion

3.1 Investigation of CO_2 and CH_4 sorption behavior in glassy polymers

As mentioned in the references, CO_2 has smaller molecular size and higher *Tc* than CH_4 [6, 16]. Also, according to the solution-diffusion model, diffusivity and solubility that are related to the size and condensability of the penetrant molecules, respectively, can affect permeability. It is clear that penetrant molecules with smaller size and higher condensability (*Tc*) have higher diffusivity and solubility and, then, higher permeability.

Table 2 and Table 3 show dual-mode sorption parameters for CO_2 and CH_4 in different glassy polymers, respectively. As can be seen, all the polymers have higher k_D, C_H', and b for CO_2 than CH_4, which can be related to higher solubility of CO_2 than CH_4 in these polymers.

Table 2: Dual mode sorption parameters and calculated parameters of different glassy polymers for CO_2

Designation	**k_D**	**C'_H**	**b**	**K**	**$P_{50/50}$**	**θ**	**lim C_D/C**	**lim C_D/C_H**	**lim C_H/C**	**S^∞**
CPI1-180	2.422	44.000	0.730	13.255	16.8	0.925	0.070	0.075	0.930	34.521
CPI1-230	1.976	45.900	0.648	15.065	21.7	0.934	0.062	0.066	0.938	31.741
6F-bisAPAF-300	1.600	11.200	0.800	5.600	5.8	0.821	0.152	0.179	0.848	10.560
6F-bisAPAF-350	1.230	30.000	0.500	12.195	22.4	0.918	0.076	0.082	0.924	16.230
6F-bisAPAF-400	1.600	35.000	0.550	12.031	20.1	0.917	0.077	0.083	0.923	20.850
6F-bisAPAF-450	1.750	43.000	0.450	11.057	22.3	0.910	0.083	0.090	0.917	21.100
PIM-1	2.351	106.796	0.421	19.124	43.1	0.948	0.050	0.052	0.950	47.312
PPO	0.849	25.865	0.240	7.296	26.3	0.863	0.121	0.137	0.879	7.044
CPPO	0.792	26.278	0.285	9.465	29.7	0.894	0.096	0.106	0.904	8.286
MeCPPO	0.652	20.613	0.268	8.465	27.9	0.882	0.106	0.118	0.894	6.175
BPPO	0.991	37.794	0.305	11.626	34.8	0.914	0.079	0.086	0.921	12.515
PS	0.650	7.700	0.370	4.383	9.1	0.772	0.186	0.228	0.814	3.499
CPI2-200	1.990	41.600	0.640	13.379	19.3	0.925	0.070	0.075	0.930	28.614
CPI2-425	2.310	70.600	0.630	19.255	29.0	0.948	0.049	0.052	0.951	46.788
CPI2-g-γ-CD-200	2.330	49.700	0.560	11.945	19.5	0.916	0.077	0.084	0.923	30.162
CPI2-g-γ-CD-425	2.650	87.700	1.100	36.404	32.2	0.973	0.027	0.027	0.973	99.120
6F-6FpDA	1.277	40.700	0.364	11.601	29.1	0.914	0.079	0.086	0.921	16.092
6F-1,5-NDA	1.380	42.800	0.930	28.843	29.9	0.965	0.034	0.035	0.966	41.184
PSF	0.630	16.503	0.356	9.326	23.4	0.893	0.097	0.107	0.903	6.505
DMPSF	0.482	12.166	0.287	7.244	21.8	0.862	0.121	0.138	0.879	3.974
BPSF	0.429	17.700	0.261	10.769	37.4	0.907	0.085	0.093	0.915	5.049
TMSPSF	0.324	20.719	0.155	9.912	57.5	0.899	0.092	0.101	0.908	3.535
PC	0.685	18.805	0.262	7.185	23.6	0.861	0.122	0.139	0.878	5.608
PH	0.289	10.010	0.184	6.373	29.2	0.843	0.136	0.157	0.864	2.131
PEI	0.758	25.020	0.366	12.081	30.3	0.917	0.076	0.083	0.924	9.915
PA	0.685	18.810	0.262	7.194	23.6	0.861	0.122	0.139	0.878	5.613
PC	0.631	22.690	0.215	7.731	31.3	0.871	0.115	0.129	0.885	5.509
6F-TADPO	1.526	34.084	1.023	22.849	21.4	0.956	0.042	0.044	0.958	36.394
BTMSPSF	0.643	15.906	0.257	6.357	20.8	0.843	0.136	0.157	0.864	4.731
6F-HAB	1.400	35.000	0.340	8.500	22.1	0.882	0.105	0.118	0.895	13.300
6F-HAB-TR-350	1.100	51.000	0.420	19.473	44.0	0.949	0.049	0.051	0.951	22.520
6F-HAB-TR-400	1.500	60.000	0.580	23.200	38.3	0.957	0.041	0.043	0.959	36.300
6F-HAB-TR-450	1.600	62.000	0.530	20.538	36.9	0.951	0.046	0.049	0.954	34.460
Ultem	1.040	17.300	0.355	5.905	13.8	0.831	0.145	0.169	0.855	7.182
Matrimid	1.440	25.500	0.367	6.499	15.0	0.846	0.133	0.154	0.867	10.799
PTMSP	1.050	130.000	0.040	4.952	98.8	0.798	0.168	0.202	0.832	6.250

The unit of k_D is (cm^3/cm^3.atm), C'_H is (cm^3/cm^{3}polymer), b is (atm^{-1}), $P_{50/50}$ is (atm) and S^∞ is (cm^3/cm^3.atm) and lim C_D/C, lim C_D/C_H, and lim C_H/C are in P=0.

Table 3: Dual mode sorption parameters and calculated parameters of different glassy polymers for CH_4

Designation	k_D	C'_H	b	K	$P_{50/50}$	θ	lim C_D/C	lim C_D/C_H	lim C_H/C	S^∞
CPI1-180	0.064	27.200	0.190	80.750	419.7	0.988	0.012	0.012	0.988	5.232
CPI1-230	0.068	25.100	0.170	62.750	363.2	0.984	0.016	0.016	0.984	4.335
6F-bisAPAF-300	0.700	3.100	0.700	3.100	3.0	0.677	0.244	0.323	0.756	2.870
6F-bisAPAF-350	0.700	11.000	0.400	6.286	13.2	0.841	0.137	0.159	0.863	5.100
6F-bisAPAF-400	0.820	18.000	0.370	8.122	19.2	0.877	0.110	0.123	0.890	7.480
6F-bisAPAF-450	1.180	20.000	0.240	4.068	12.8	0.754	0.197	0.246	0.803	5.980
PIM-1	0.592	64.966	0.150	16.461	103.1	0.939	0.057	0.061	0.943	10.337
PPO	0.267	19.101	0.108	7.693	62.1	0.870	0.115	0.130	0.885	2.325
CPPO	0.298	15.531	0.125	6.533	44.1	0.847	0.133	0.153	0.867	2.246
MeCPPO	0.270	10.106	0.124	4.637	29.4	0.784	0.177	0.216	0.823	1.521
BPPO	0.418	24.935	0.151	9.025	53.0	0.889	0.100	0.111	0.900	4.193
PS	0.175	2.530	0.146	2.111	7.6	0.526	0.321	0.474	0.679	0.544
CPI2-200	0.497	14.196	0.143	4.078	21.6	0.755	0.197	0.245	0.803	2.524
CPI2-425	0.641	20.148	0.181	5.679	25.9	0.824	0.150	0.176	0.850	4.284
CPI2-g-γ-CD-200	0.551	14.315	0.154	4.010	19.5	0.751	0.200	0.249	0.800	2.761
CPI2-g-γ-CD-425	0.787	40.149	0.200	10.198	46.0	0.902	0.089	0.098	0.911	8.808
6F-6FpDA	0.287	20.630	0.117	8.410	63.3	0.881	0.106	0.119	0.894	2.701
6F-1,5-NDA	0.330	27.580	0.140	11.701	76.4	0.915	0.079	0.085	0.921	4.191
PSF	0.167	9.044	0.118	6.390	45.7	0.844	0.135	0.156	0.865	1.234
DMPSF	0.078	7.348	0.108	10.174	84.9	0.902	0.089	0.098	0.911	0.872
BPSF	0.096	8.810	0.084	7.709	79.9	0.870	0.115	0.130	0.885	0.836
TMSPSF	0.199	8.299	0.090	3.753	30.6	0.734	0.210	0.266	0.790	0.946
PC	0.147	8.382	0.084	4.786	45.0	0.791	0.173	0.209	0.827	0.852
PH	0.051	2.700	0.067	3.547	38.0	0.718	0.220	0.282	0.780	0.232
PEI	0.207	7.310	0.136	4.803	28.0	0.792	0.172	0.208	0.828	1.201
PA	0.147	8.380	0.084	4.789	45.1	0.791	0.173	0.209	0.827	0.851
PC	0.181	6.450	0.100	3.564	25.6	0.719	0.219	0.281	0.781	0.826
6F-TADPO	0.327	22.838	0.160	11.175	63.6	0.911	0.082	0.089	0.918	3.981
BTMSPSF	0.211	9.375	0.105	4.665	34.9	0.786	0.177	0.214	0.823	1.195
6F-HAB	0.440	11.000	0.110	2.750	15.9	0.636	0.267	0.364	0.733	1.650
6F-HAB-TR-350	0.340	23.000	0.130	8.794	60.0	0.886	0.102	0.114	0.898	3.330
6F-HAB-TR-400	0.460	32.000	0.180	12.522	64.0	0.920	0.074	0.080	0.926	6.220
6F-HAB-TR-450	0.490	36.000	0.160	11.755	67.2	0.915	0.078	0.085	0.922	6.250
Ultem	0.170	5.830	0.210	7.202	29.5	0.861	0.122	0.139	0.878	1.394
Matrimid	0.136	14.30	0.105	11.040	95.6	0.909	0.083	0.091	0.917	1.638
PTMSP	0.500	62.000	0.050	6.200	104.0	0.839	0.139	0.161	0.861	3.600

The unit of k_D is (cm^3/cm^3.atm), C'_H is (cm^3/cm^3polymer), b is (atm^{-1}), $P_{50/50}$ is (atm) and S^∞ is (cm^3/cm^3.atm) and lim C_D/C, lim C_D/C_H, and lim C_H/C are in P=0.

As mentioned above, CO_2 has smaller molecular size than CH_4 and can quickly saturate Langmuir sites and then immediately start to occupy Henry sites (higher k_D); however, CH_4 needs higher pressure to saturate Langmuir sites. As can be seen in Eq. (7) and Eq. (8), increasing the pressure in the dual-mode sorption leads to a decrease in the Langmuir sorption to the total sorption ratio up to zero and increase the Henry sorption to the total sorption ratio up to one.

$$\lim_{P\to\infty}\frac{C_H}{C}=0 \tag{7}$$

$$\lim_{P\to\infty}\frac{C_D}{C}=1 \tag{8}$$

These two equations confirmed that, for CO_2, by increasing the pressure, Langmuir sites are saturated very fast and, afterwards, the Henry sorption is dominant. However, CH_4 could not easily enter the Langmuir site, which could make the Langmuir sorption significant up to high pressure. According to the sorption curves for the Langmuir and Henry sorption, at the beginning, penetrant molecules are motivated to occupy the Langmuir sites and to fill these pores and, at low pressure for most of the penetrant in the polymers, Langmuir sorption is dominant. After a while, due to the saturation of most of the Langmuir sites, the sorption of the penetrant molecules in the Langmuir site become more difficult, this resulted in an increase of the sorption in Henry sites.

The infinite dilution solubility coefficient (S^∞) from the dual-mode sorption model given by Eq. (9) represents the solubility coefficient in the limit of zero concentration (very low pressure) [16]. Table 2 and Table 3 list the values of S^∞ for CO_2 and CH_4, respectively.

$$S^\infty=\lim_{P\to 0}S=\lim_{P\to 0}\left(k_D+\frac{C'_H b}{1+bp}\right)=k_D+C'_H b=k_D\left(1+K\right) \tag{9}$$

This parameter can be a piece of good evidence for the solubility of penetrant in special polymers. Comparison of this parameter for special penetrant in different polymers shows the polymers with higher solubility for that penetrant. While the gas sorption at low pressures tends to be dominated by the non-equilibrium nature of glassy polymers (Langmuir site) and $C_H'b$ is much higher than k_D at very low pressures, S^∞ is equal to $C_H'b$. As pressure increased, the solubility coefficients are reduced, especially for the more condensable gases [16].

3.2 $P_{50/50}$ parameter

$P_{50/50}$ is the pressure with an equal sorption amount in Henry and Langmuir sites. This parameter is defined to compare the difference of sorption in various polymers and can be calculated by Eq. (10).

$$\text{At } P_{50/50}\text{: } C_D=C_H \Rightarrow k_D P_{50/50}=\frac{C'_H b p_{50/50}}{1+bp_{50/50}} \Rightarrow P_{50/50}=\frac{C'_H b-k_D}{bk_D}=\frac{K-1}{b} \tag{10}$$

Table 2 and Table 3 show the calculated amount of this parameter for CO_2 and CH_4, respectively. As can be seen in Figure 3 and Figure 4, this pressure is lower for CO_2 than it is for CH_4, showing that at the low pressure, the contribution of the Langmuir sorption to the total sorption is higher. However, for some polymers, this pressure is very high, which cannot be covered by the sorption data and the Langmuir sorption is always dominant. Higher $P_{50/50}$ means that the Langmuir sorption is more important than the Henry sorption. This parameter can be used to make a decision about the sorption model. For extremely small $P_{50/50}$, the sorption model is near the Henry sorption and, for very high $P_{50/50}$, the sorption model is close to the Langmuir sorption.

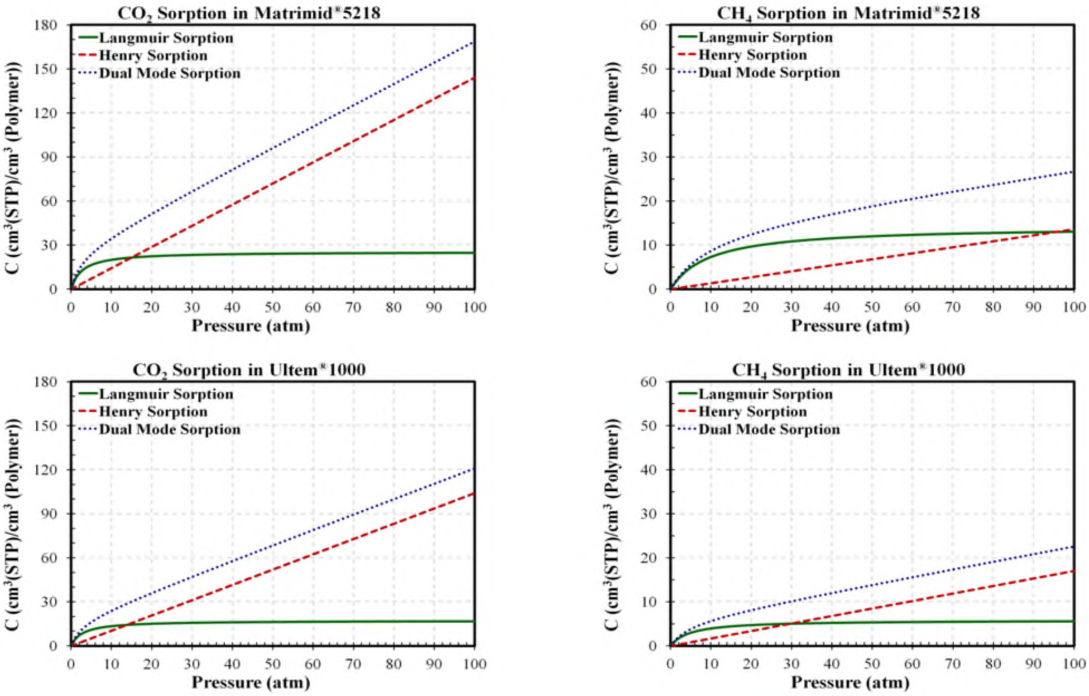

Fig.3: Henry, Langmuir and Dual mode sorption isotherms for CO_2 and CH_4 in Matrimid®5218 and Ultem®1000 @ 35ºC

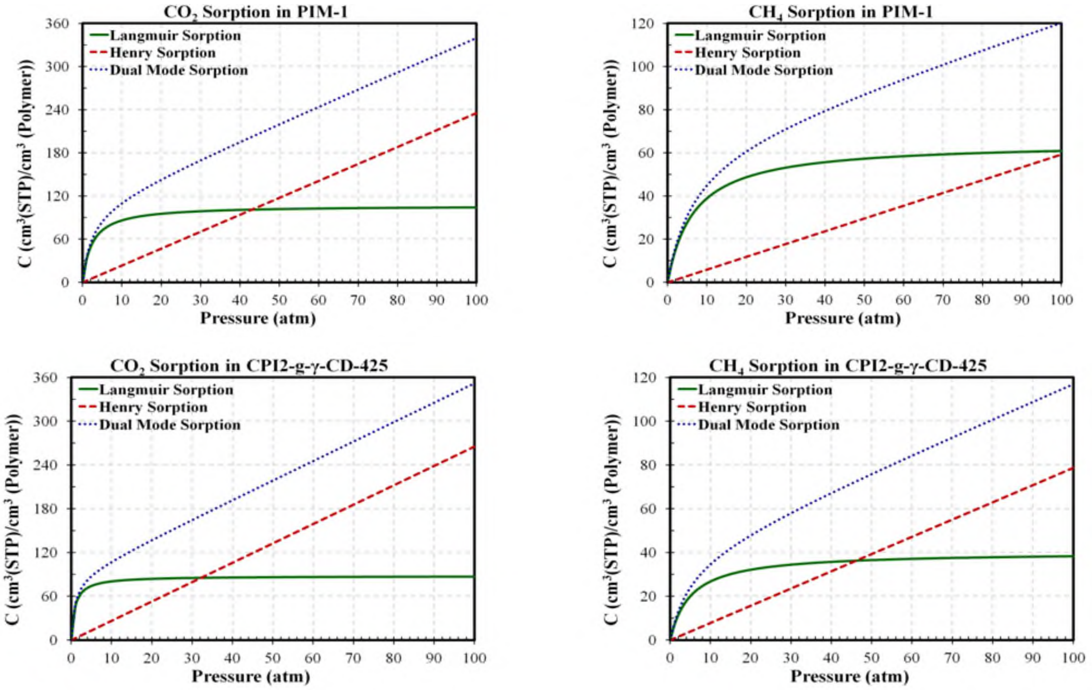

Fig.4: Henry, Langmuir and Dual mode sorption isotherms for CO_2 and CH_4 in PIM-1 and CPI2-g-γ-CD-425 @ 35ºC

3.3 Saturated percentage of Langmuir sites in $P_{50/50}$ (θ)

Saturated percentage of Langmuir sites is crucial due to the effect of pressure on sorption and permeation. This parameter shows the extent to which Langmuir sites are saturated at $P_{50/50}$. The higher this parameter, the faster the sorption of penetrant is in Langmuir sites and the more the

Langmuir sorption is sensitive to pressure. Moreover, the sorption also occurs at low pressures. The saturated percentage of Langmuir sites at $P_{50/50}$ can be calculated by Eq. (11).

$$\theta = \frac{C_H\ @\ p : p_{50/50}}{C_H\ @\ p : p_{\inf.}} = \frac{\dfrac{C'_H b p_{50/50}}{\left(1+bp_{50/50}\right)}}{\dfrac{C'_H b p_{\inf.}}{\left(1+bp_{\inf.}\right)}} = \frac{\dfrac{C'_H b \dfrac{\left(C'_H b - k_D\right)}{bk_D}}{1+b\dfrac{\left(C'_H b - k_D\right)}{bk_D}}}{C'_H} = \frac{C'_H b - k_D}{C'_H b} = 1 - \frac{k_D}{C'_H b} = 1 - \frac{1}{K} \tag{11}$$

According to the shape of the sorption curve, it is obvious that the Langmuir mode is more sensitive to pressure than the Henry mode; based on the results of Table 2 and Table 3, most of the Langmuir sites are usually saturated at $P_{50/50}$. Therefore, a small amount of difference at $P_{50/50}$ is crucial. Other important parameters calculated in Table 2 and Table 3 is the Henry sorption to the Langmuir sorption (Eq. (12)) as well as the Henry sorption to the total sorption ratio both at zero pressure (Eq. (13)).

$$\lim_{P\to 0}\frac{C_D}{C_H} = \lim_{P\to 0}\frac{k_D p}{\dfrac{C'_H bp}{1+bp}} = \frac{k_D}{C'_H b} = \frac{1}{K} \tag{12}$$

$$\lim_{P\to 0}\frac{C_D}{C} = \lim_{P\to 0}\frac{k_D p}{k_D p + \dfrac{C'_H bp}{1+bp}} = \frac{k_D}{k_D + C'_H b} = \frac{1}{1+K} \tag{13}$$

As mentioned previously, K is a dimensionless variable that is related to all dual-mode sorption parameters. Figure 3 and Figure 4 show CO_2 and CH_4 sorption as functions of pressure in Henry and Langmuir sites for different polymers, respectively. Moreover, Figure 5 and Figure 6 demonstrate the contributions of Henry and Langmuir sorption as functions of pressure for different polymers, respectively.

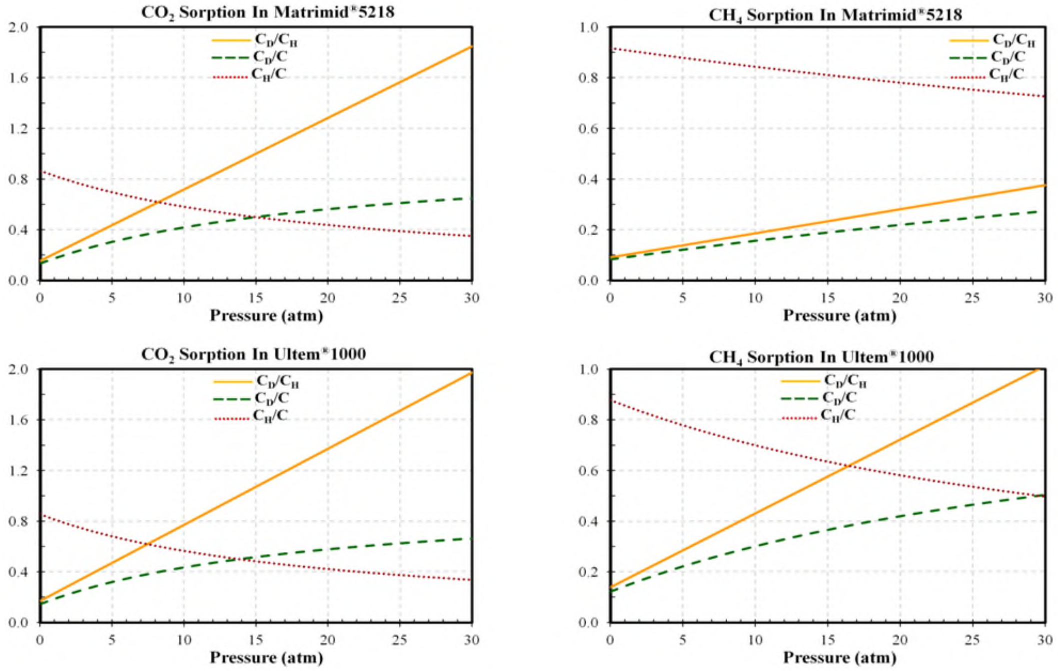

Fig.5: Contribution of Henry and Langmuir sorption from total sorption for CO_2 and CH_4 in Matrimid®5218 and Ultem®1000

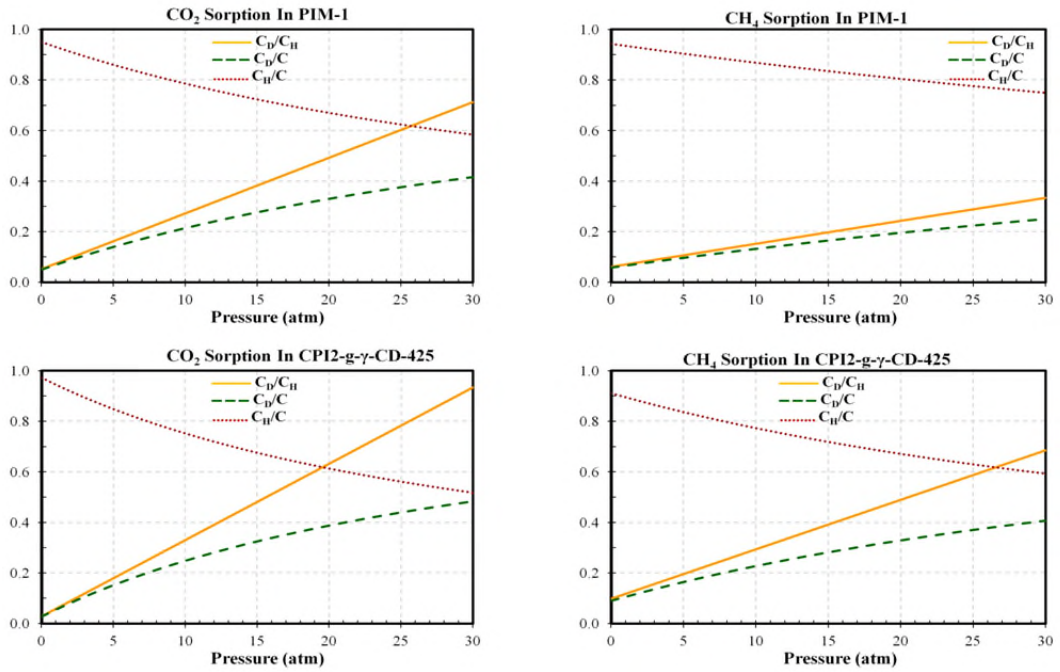

Fig.6: Contribution of Henry and Langmuir sorption from total sorption for CO$_2$ and CH$_4$ in PIM-1 and CPI2-g-γ-CD-425

3.4 Analysis of partial immobilization model

As mentioned before, the partial immobilization model is based on the independent dual diffusion of the Henry and Langmuir modes. However, it assumes that species in the Langmuir mode can relatively mobilize in glassy polymeric membranes and *F* factor is the portion of mobile sorbed penetrant in Langmuir sites. The amount of *F* factor ranges from 0.01 to 0.2 for different penetrants in various polymers, showing that the portion of the Langmuir sorption is less than 20 percent of the total sorption. Researchers have defined *F* factor as D_H/D_D and assumed this amount to correspond to $C_{Hmobile}/C_H$, meaning that the portion of the concentration of mobile molecules in the Langmuir site corresponds to the ratio of diffusivity in the Langmuir site to the Henry site [39-41]. This assumption is correct under particular conditions. In general, these two definitions for *F* factor are different from one another. To show the difference between these two definitions, two parameters F_C and F_D are defined as below.

$$F_C = \frac{C_{H_{mobile}}}{C_H} \tag{14}$$

$$F_D = \frac{D_H}{D_D} \tag{15}$$

Generally, the penetrant concentrations are divided into mobile and immobile concentrations. Mobile concentration and diffusivity coefficient are defined as C_m and *D*, respectively, and the immobile concentration is defined as C-C_m. Thus, the mobile and immobile concentrations can be defined as Eq. (16) and Eq. (17).

$$\text{Mobile Concentration}: C_m = C_D + F_C C_H = k_D p + F_C\left(\frac{C'_H bp}{1+bp}\right) \tag{16}$$

$$\text{Immobile Concentration}: C - C_m = (1 - F_C)C_H = (1 - F_C)\left(\frac{C'_H bp}{1+bp}\right) \tag{17}$$

The permeation flux through the membrane can be written in two conditions. In the first one, two diffusion coefficients are defined for Henry sites (D_D) and Langmuir sites (D_H) and the driving force is total concentration (C). In the second condition, the diffusion coefficients of both Langmuir and Henry sites are the same (D), but the driving force is only mobile concentration ($C_{Hmobile}$). Eq. (18) and Eq. (19) show the permeation flux in these two conditions. As can be seen in these two equations, if $D=D_D$ and $F_C=F_D$, these two permeation fluxes are equal.

$$J=-D_D\frac{\partial C_D}{\partial y}-D_H\frac{\partial C_H}{\partial y}=-D_D\frac{\partial C_D}{\partial p}\cdot\frac{\partial p}{\partial y}-D_H\frac{\partial C_H}{\partial p}\cdot\frac{\partial p}{\partial y}=-D_D\left(\frac{\partial C_D}{\partial p}-F_D\frac{\partial C_H}{\partial p}\right)\frac{\partial p}{\partial y} \tag{18}$$

$$J=-D\frac{\partial C_D}{\partial y}-D\frac{\partial C_{H_{mobile}}}{\partial y}=-D\frac{\partial C_D}{\partial p}\cdot\frac{\partial p}{\partial y}-D\frac{\partial\left(F_C\cdot C_H\right)}{\partial p}\cdot\frac{\partial p}{\partial y}=-D\left(\frac{\partial C_D}{\partial p}-F_C\frac{\partial C_H}{\partial p}\right)\frac{\partial p}{\partial y} \tag{19}$$

To show the difference of these two conditions, the permeation flux and permeability coefficient can be written as shown below:

$$J=-D_D\frac{\partial C_D}{\partial y}-D_H\frac{\partial C_{H_{mobile}}}{\partial y}=-D_D\frac{\partial C_D}{\partial p}\cdot\frac{\partial p}{\partial y}-D_H\frac{\partial\left(F_C\cdot C_H\right)}{\partial p}\cdot\frac{\partial p}{\partial y} \tag{20}$$

$$C_m=C_D+F_CC_H=k_Dp+F_C\frac{C'_Hbp}{1+bp} \tag{21}$$

$$J=-D_D\frac{\partial C_D}{\partial p}\cdot\frac{\partial p}{\partial y}-D_H\frac{\partial\left(F_C\cdot C_H\right)}{\partial p}\cdot\frac{\partial p}{\partial y}=\left(-k_DD_D-D_HF_C\frac{C'_Hbp}{\left(1+bp\right)^2}\right)\cdot\frac{\partial p}{\partial y} \tag{22}$$

$$J=\left(-k_DD_D-D_HF_C\frac{C'_Hbp}{\left(1+bp\right)^2}\right)\cdot\frac{\partial p}{\partial y}=-k_DD_D\left(1+\frac{F_DF_C\frac{C'_Hb}{k_D}}{\left(1+bp\right)^2}\right)\cdot\frac{\partial p}{\partial y} \tag{23}$$

$$P=-\frac{\left(\int_0^L J\cdot dy\right)}{\Delta p}=\frac{\int_{p_1}^{p_2}k_D\cdot D_D\left(1+\frac{F_DF_C\frac{C'_Hb}{k_D}}{\left(1+bp\right)^2}\right)\cdot\partial p}{\Delta p}=k_DD_D\left(1+\frac{F_DF_CK}{(1+bp)}\right) \tag{24}$$

As can be seen, if $F=F_C\times F_D$, then Eq. (24) is equal to Eq. (4) ,which has been used in most of the references. An important point that is not analyzed cautiously in the partial immobilized model is the portion of penetrant sorption in the Langmuir site to the total sorption. Most scholars use the first condition mentioned above, in which the diffusivity coefficient in Henry sites (D_D) is always much higher than the diffusivity coefficient in Langmuir sites (D_H). In addition, F factor ranges from 0.02 to 0.2.

In order to compare and analyze the contribution of mobile molecules of the Langmuir site from the total sorption, all the polymers in Tables 4 were evaluated and figures were plotted according to the *F* factor in each reference.

Table 4: Diffusivity parameters of different glassy polymers for CO_2 and CH_4

Designation	**CO_2**			**CH_4**			**Ref.**
	D_D*10^8 (cm^2/s)	**D_H*10^8 (cm^2/s)**	**F**	**D_D*10^8 (cm^2/s)**	**D_H*10^8 (cm^2/s)**	**F**	
PIM-1	1296.600	34.120	0.026	364.000	3.340	0.009	[16]
CPI2-200	97.500	3.030	0.031	19.300	0.980	0.051	[21]
CPI2-425	507.000	24.300	0.048	78.300	5.140	0.066	[21]
CPI2-g-γ-CD-200	96.500	2.650	0.027	19.400	1.130	0.058	[21]
CPI2-g-γ-CD-425	1317.000	79.200	0.060	183.800	15.400	0.084	[21]
6F-6FpDA	25.500	1.530	0.060	2.7800	0.236	0.085	[22]
6F-1,5-NDA	10.100	0.655	0.065	0.883	0.033	0.037	[23]
PSF	4.790	0.581	0.121	0.692	0.106	0.153	[24]
DMPSF	2.846	0.452	0.159	0.520	0.051	0.098	[24]
BPSF	4.718	0.674	0.143	0.652	0.082	0.126	[25]
TMSPSF	30.973	1.202	0.039	3.521	0.221	0.063	[25]
PC	6.220	0.485	0.078	1.090	0.126	0.115	[26]
6F-TADPO	11.960	1.004	0.084	1.120	0.029	0.026	[40]
BTMSPSF	8.502	0.327	0.038	3.980	0.087	0.022	[41]

For example, the results of two commercials and two synthesized polyimide are shown in Figure 7 and Figure 8, respectively. These figures demonstrate the ratio of sorbed mobile molecules in the Langmuir site to the total sorption in the polymer for CO_2 and CH_4. In addition, the ratio of this molecule was drawn in proportion to the total mobile molecules and to Henry site molecules. The results of various polymers indicated that the contribution of mobile molecules in the Langmuir state to the total sorbed molecules in the polymer is not more than 5%, which is very small in value. However, these molecules should not be considered unimportant, because the contribution of this ratio to the total mobile molecules ranged from 5 to 70% for different polymers at low pressures, which was a considerable contribution. If the contribution of these molecules were measured compared with the sorbed molecules in the Henry site, it can be seen that, despite the existing subjective perception that the sorbed molecules in the Henry site have the main contribution in permeation, the contribution of these molecules at low pressures is not only comparable, but also up to about 1.5 times more than that of the sorbed molecules in the Henry site (in some polymers).As is clear, the contribution of these molecules rapidly disappears with increasing the pressure, which is clearly evident for CO_2. However, the mobile molecules in the Langmuir site have a significant contribution up to 11-15 atm for CH_4, considering the importance of sorption in the Langmuir sorption model. The other difference that can be seen in the contribution of these molecules to CO_2 and CH_4 is that the difference between the ratios of these molecules to the total mobile molecules from the ratio of these molecules to the molecules in the Henry site is very high for CO_2 at the initial pressure. However, this initial difference for CH_4 is not more than 0.015-0.1. The interesting point is that, despite the large initial difference between these two ratios, this difference quickly decreases with increasing the pressure. In addition, the two curves coincided at a not very high pressure. However, that small difference for CH_4 is maintained at high pressures and the difference reduction occurs very slowly.

The next case is that the contribution of mobile CO_2 molecules in the Langmuir site is more than the same amounts for CH_4 in a certain polymer to the total mobile molecules. However, by increasing pressure, for CO_2 its importance is reduced much faster than CH_4.

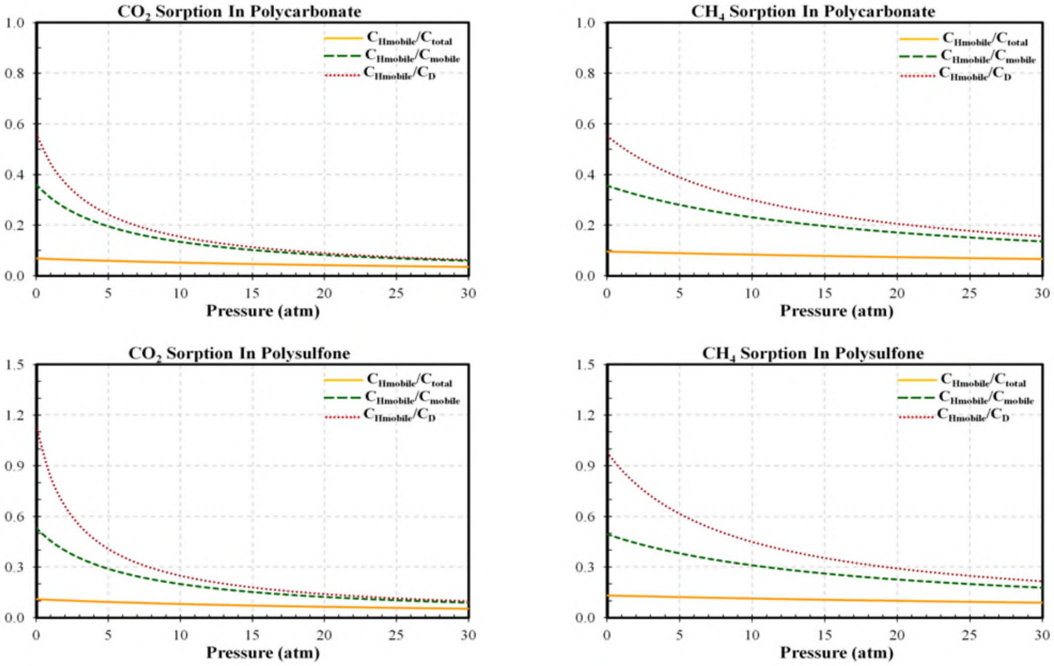

Fig.7: Contribution of mobile Langmuir sorption from total sorption for CO_2 and CH_4 in Polycarbonate and Polysulfone

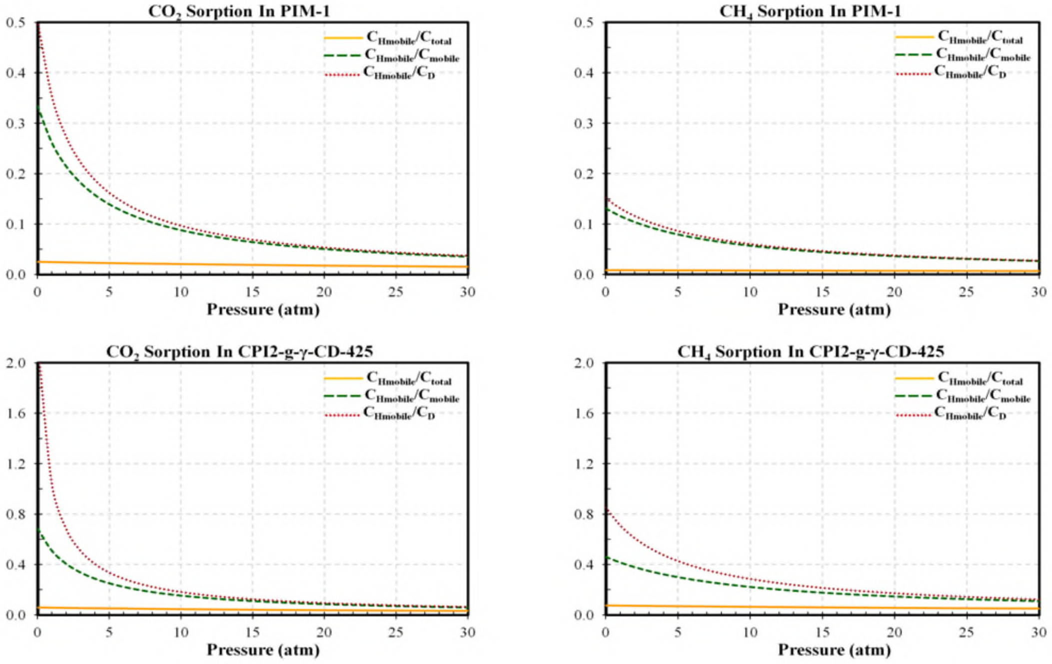

Fig.8: Contribution of mobile Langmuir sorption from total sorption for CO_2 and CH_4 in PIM-1 and CPI2-g-γ-CD-425

4. Conclusion

Investigation on the solubility of CO_2 and CH_4 in various polymers with the dual-mode sorption model showed that the sorption model of these gasses was different in terms of appearance within the normal range of sorption tests in addition to the difference in solubility. $P_{50/50}$ parameter was much smaller for the sorption of CO_2 than CH_4 in various polymers, showing that the sorption contribution in the Langmuir site was less important than the Henry site. This parameter can be used as a scale of closeness of sorption model to the pure Henry model or the pure Langmuir model. This study attempted to provide a correct definition of F factor, used in references, in the form of the multiplication of mobile concentration ratios ($C_{Hmobile}/C_H$) by the diffusivity coefficients in two modes (D_H/D_D). In addition, the contribution of each sorption mode from the total sorption as well as its impact on the permeation flux of the total membrane was determined. Meanwhile, a better description was tried to be achieved for the partial immobilization model.

5. Nomenclature

b: Langmuir affinity constant (atm $^{-1}$)
C: Total sorption amount of polymer (cm^3 gas (STP) /cm^3 polymer)
C_D: Concentrations of the penetrant sorbed at the Henry site (cm^3 gas (STP) /cm^3 polymer)
C_H: Concentrations of the penetrant sorbed at the Langmuir site (cm^3 gas (STP) /cm^3 polymer)
C'_H: Langmuir saturation constant (cm^3 gas (STP) /cm^3 polymer)
D: Average diffusivity coefficient (cm^2/s)
$D(C)$: Concentration dependent diffusion coefficient (cm^2/s)
D_D: Henry's law diffusion coefficient (cm^2/s)
D_H: Langmuir mode diffusion coefficient (cm^2/s)
F: Mobile fraction of the Langmuir mode species
J: permeation flux (cm^3 gas (STP) / s)
k_D: Henry's solubility coefficient ((cm^3 gas (STP)) / (cm^3 polymer-atm))
p: Pressure of the feed (atm)
P: Average permeability coefficient (Barrer)
S: Solubility coefficient ((cm^3 gas (STP)) / (cm^3 polymer-atm))
y: Polymer thickness (cm)

References

[1] Kraftschik, B., Koros, W.J., Johnson, J.R., Karvan, O. (2013). Dense film polyimide membranes for aggressive sour gas feed separations. Journal of Membrane Science, vol. 428, p. 608-619.

[2] Askari, M., Yang, T., Chung, T.S. (2012). Natural gas purification and olefin/paraffin separation using cross-linkable dual-layer hollow fiber membranes comprising β-cyclodextrin. Journal of Membrane Science, vol. 423-424, p. 392-403.

[3] White, L.S., Blinka, T.A., Kloczewski, H.A., Wang, I.F. (1995). Properties of a polyimide gas separation membrane in natural gas streams. Journal of Membrane Science, vol. 103, no. 1-2, p. 73-82.

[4] Xiao, Y.C., Low, B.T., Hosseini, S.S., Chung, T.S., Paul, D.R. (2009). The strategies of molecular architecture and modification of polyimide based membranes for CO2 removal from natural gas-A review. Progress in Polymer Science, vol. 34, no. 6, p. 561-580.

[5] Kim, S., Jo, H.J., Lee, Y.M. (2013). Sorption and transport of small gas molecules in thermally rearranged (TR) polybenzoxazole membranes based on 2,2-bis(3-amino-4-hydroxyphenyl)-hexafluoropropane (bisAPAF) and 4,4'-hexafluoroisopropylidene diphthalic anhydride (6FDA) . Journal of Membrane Science, vol. 441, p. 1-8.

[6] Askari, M., Xiao, Y.C., Li, P., Chung, T.S. (2012). Natural gas purification and olefin/paraffin separation using cross-linkable 6FDA-Durene/DABA co-polyimides grafted with α, β, and γ-cyclodextrin. Journal of Membrane Science, vol. 390-391, p. 141-151.

[7] Mi, Y., Stern, S.A., Trohalaki, S. (1993). Dependence of the gas permeability of some polyimide isomers on their intrasegmental mobility. Journal of Membrane Science, vol. 77, no. 1, p. 41-48.

[8] Hirayama, Y., Yoshinaga, T., Kusuki, Y., Ninomiya, K., Sakakibara, T., Tamari, T. (1996). Relation of gas permeability with structure of aromatic polyimides I. Journal of Membrane Science, vol. 111, no. 2, p. 169-182.

[9] Jung, C.H., Lee, Y.M. (2008). Gas permeation properties of hydroxyl-group containing polyimide membranes. Macromolecular Research, vol. 16, no. 6, p. 555-560.

[10] Coleman, M.R., Koros, W.J. (1990). Isomeric polyimides based on fluorinated dianhydrides and diamines for gas separation applications. Journal of Membrane Science, vol. 50, no. 3, p. 285-297.

[11] Tanaka, K., Kita, H., Okano, M., Okamoto, K.I. (1992). Permeability and permselectivity of gases in fluorinated and non-fluorinated polyimides. Polymer, vol. 33, no. 3, p. 585-592.

[12] Bickel, C.S., Koros, W.J. (1999). Improvement of CO2/CH4 separation characteristics of polyimides by chemical crosslinking. Journal of Membrane Science, vol. 155, no. 1, p. 145-154.

[13] Sanders, D.F., Smith, Z.P., Guo, R., Robeson, L.M., McGrath, J.E., Paul, D.R., Freeman, B.D. (2013). Energy-efficient polymeric gas separation membranes for a sustainable future: A review. Polymer, vol. 54, no. 18, p. 4729-4761.

[14] Budd, P.M., Msayib, K.J., Tattershall, C.E., Ghanem, B.S., Reynolds, K.J., McKeown, M.B., Fritch, D. (2005). Gas separation membrane from polymer of intrinsic microscopy. Journal of Membrane Science, vol. 251, no. 1-2, p. 263-269.

[15] Kita, H., Inada, T., Tanaka, K., Okamoto, K. (1994). Effect of photocrosslinking on permeability and permoselectivity of gases through benzophenone-containing polyimide. Journal of Membrane Science, vol. 87, no. 1-2, p. 139-147.

[16] Li, P., Chung, T.S., Paul, D.R. (2013). Gas sorption and permeation in PIM-1. Journal of Membrane Science, vol. 432, p. 50-57.

[17] Lau, C.H., Li, P., Li, F.Y., Chung, T.S., Paul, D.R. (2013). Reverse-selective polymeric membranes for gas separations. Progress In Polymer Science, vol. 38, no. 5, p. 740-766.

[18] Story, B.J., Koros, W.J. (1992). Sorption and transport of CO2 and CH4 in chemically modified poly (phenylene oxide). Journal of Membrane Science, vol. 67, no. 2-3, p. 191-210.

[19] Paul, D.R. (1979). Gas sorption and transport in glassy polymers. Ber. Bunsenges Phys. Chem., vol. 83, no. 4, p. 294-302.

[20] Vieth, W.R., Frangoulis, C.S., Rionda, J.A. (1966). Kinetics of sorption of methane in glassy polystyrene. Journal of Colloid and Interface Science, vol. 22, no. 5, p. 454-461.

[21] Askari, M., Chua, M.L., Chung, T.S. (2014). Permeability, solubility, diffusivity and PALS data of cross-linkable 6FDA-based copolyimides. Industrial and Engineering Chemistry Research, vol. 53, no. 6, p. 2449-2460.

[22] Wang, R., Cao, C., Chung, T.S. (2002). A critical review on diffusivity and the characterization of diffusivity of 6FDA-6FpDA polyimide membranes for gas separation. Journal of Membrane Science, vol. 198, no. 2, p. 259-271.

[23] Wang, R., Chan, S.S., Liu, Y., Chung, T.S. (2002). Gas transport properties of poly (1,5-naphthalene-2,2_bis(3,4-phthalic) hexafluoropropane) diimide (6FDA-1,5-NDA) dense membranes. Journal of Membrane Science, vol. 199, no. 1-2, p. 191-202.

[24] Kim, H.J., Hong, S.I. (1997). Sorption and permeation of CO2 and CH4 for dimethylated polysulfone membrane. Korean Journal of Chemical Engineering, vol. 14, no. 3, p. 168-174.

[25] Kim, H.J., Hong, S.I. (1997). The transport properties of CO2 and CH4 for brominated polysulfone membrane. Korean Journal of Chemical Engineering, vol. 16, no. 3, p. 343-350.

[26] Koros, W.J., Chan, A.H., Paul, D.R. (1997). Sorption and transport of various gases in polycarbonatem membrane. Journal of Membrane Science, vol. 2, p. 165-190.

[27] Barbari, T.A., Koros, W.J., Paul, D.R. (1988). Gas sorption in polymers based on bisphenol-A. Journal of Polymer Science: Part B: Polymer Physics, vol. 26, no. 4, p. 729-744.

[28] Koros, W.J., Fleming, G.K., Jordan, S.M., Kim, T.H., Hoehn, H.H. (1988). Polymeric membrane materials for solution-diffusion based permeation separations. Progress in Polymer Science, vol. 13, no. 4, p. 339-401.

[29] Paul, D.R., Koros, W.J. (1976). Effect of partially immobilizing sorption on permeability and the diffusion time lag. Journal of Polymer Science: Part B: Polymer Physics, vol. 14, no. 4, p. 675-685.

[30] Lin, W.H., Chung, T.S. (2001). Gas permeability, diffusivity, solubility, and aging characteristics of 6FDA-durene polyimide membranes. Journal of Membrane Science, vol. 186, no. 2, p. 183-193.

[31] Tsujita, Y. (2003). Gas sorption and permeation of glassy polymers with microvoids. Progress in Polymer Science, vol. 28, no. 29, p. 1377-1401.

[32] Koros, W.J., Hellums, M.W. (1989). Gas separation membrane material selection criteria: differences for weakly and strongly interaction feed components. Fluid Phase Equilibria, vol. 53, p. 339-354.

[33] Koros, W.J., Chern, R.T., Stannett, V.T., Hopfenberg, H.B. (1981). A model for permeation of mixed gases and vapors in glassy polymers. Journal of Polymer Science: Part B: Polymer Physics, vol. 19, no. 10, p. 1513-1530.

[34] Kanehashi, S., Nagai, K. (2005). Analysis of dual-mode model parameters for gas sorption in glassy polymers Journal of Membrane Science, vol. 253, no. 1-2, p. 117-138.

[35] Bonder, V.I., Kamiya, Y., Yampol‘skii, Y.P. (1996). On Pressure Dependence of the Parameters of the Dual-Mode Sorption Model. Journal of Polymer Science: Part B: Polymer Physics, vol. 34, no. 2, p. 369-378.

[36] Toi, K., Morel, G., Paul, D.R. (1982). Gas sorption and transport in poly (phenylene oxide) and comparisons with other glassy polymers. Journal of Applied Polymer Science, vol. 27, no. 8, p. 2997-3005.

[37] Ranade, G.R., Chandler, R., Plank, C.A., Laukhuf, W.L.S. (1985). Evidence of dual mobility in sulfur dioxide–polyarylate system: an integral sorption analysis. Polymer Engineering and Science, vol. 25, no. 3, p. 164-169.

[38] Bos, A., Punt, I.G.M., Wessling, M., Strathmann, H. (1999). CO2-induced plasticization phenomena in glassy polymers. Journal of Membrane Science, vol. 155, no. 1, p. 67-78.

[39] Ahmad, A.L., Adewole, J.K., Leo, C.P., Ismail, S., Sultan, A.S., Olatunji, S.O. (2015). Prediction of plasticization pressure of polymeric membranes for CO2 removal from natural gas. Journal of Membrane Science, vol. 480, p. 39-46.

[40] Al-Juaied, M., Koros, W.J. (2005). Frame of reference effects on the performance of hollow fiber membranes. Industrial and Engineering Chemistry Research, vol. 44, no. 10, p. 3648-3654.

[41] Kim, H.J., Hong, S.I. (2000). Gas permeabilities of CO2 and CH4 for polysulfones substituted with bromo and trimethylsilyl Groups. Korean Journal of Chemical Engineering, vol. 17, no. 1, p. 122-127.

[42] Smith, Z.P., Sanders, D.F., Ribeiro, C.P., Guo R., Freeman, B.D., Paul, D.R., McGrath, J.E., Swinnea, S. (2012). Gas sorption and characterization of thermally rearranged polyimides based on 3,3'-dihydroxy-4,4'-diamino-biphenyl (HAB) and 2,2'-bis-(3,4-dicarboxyphenyl) hexafluoropropane dianhydride (6FDA). Journal of Membrane Science, vol. 415-416, p. 558-567.

[43] Sanders, D.F., Guo, R., Smith, Z.P., Stevens, K.A., Liu, Q., McGrath, J.E., Paul, D.R., Freeman, B.D. (2014). Influence of polyimide precursor synthesis route and ortho-position functional group on thermally rearranged (TR) polymer properties: Pure gas permeability and selectivity. Journal of Membrane Science, vol. 463, p. 73-81.

[44] Moore, T.T., Koros, W.J. (2007). Gas sorption in polymers, molecular sieves, and mixed matrix membranes. Journal of Applied Polymer Science, vol. 104, no. 6, p. 4053-4059.

[45] Vu, D.Q., Koros, W.J., and Miller, S.J. (2003). Mixed matrix membranes using carbon molecular sieves I. Preparation and experimental results. Journal of Membrane Science, vol. 211, no. 2, p. 311-334.

[46] Plate, N.A., Bokarev, A.K., Kaliuzhnyi, N.E., Litvinova, E.G., Khotimskii, V.S., Volkov, V.V., Yampol‘skii, Y.P. (1991). Gas and vapor permeation and sorption in poly (trimetylsilylpropyne). Journal of Membrane Science, vol. 60, no. 1, p. 13-24.

[47] Gomes, D., Nunes, S.P., Peinemann, K.V. (2005). Membranes for gas separation based on poly (1-trimethylsilyl-1-propyne)-silica nanocomposites. *Journal of Membrane Science*, vol. 246, no. 1, p. 13-25.